THE AMERICAN SOCIETY OF MECHANICAL ENGINEERS
345 E. 47th St., New York, N.Y. 10017

95-GT-434

A NEW METHOD FOR THE PREDICTION OF COMPRESSOR PERFORMANCE MAPS USING ONE-DIMENSIONAL ROW-BY-ROW ANALYSIS

Magdy S. Attia and M. Taher Schobeiri
Department of Mechanical Engineering
Texas A&M University
College Station, Texas

ABSTRACT

This article presents a new and simple method for the prediction of the compressor performance maps based on the geometry and the design point data. The method accurately calculates the compressor performance map based on a comprehensive one-dimensional row-by-row analysis. Off-design efficiency is determined using a modified diffusion factor and an advanced loss calculation method that allows for the accurate prediction of the operational characteristics of the compressor in the post-stall regime. Three different compressor performance maps are generated for low, intermediate and high pressure stage groups using the geometry of the multistage compressor of a power generation gas turbine engine. The results are compared with the maps obtained from experiment.

NOMENCLATURE

b	=	blade height
D	=	diffusion factor, diameter
H, h	=	specific total, static enthalpy
l	=	specific stage mechanical energy
$\dot{m}$	=	mass flow rate
r	=	degree of reaction
R	=	radius, density ratio
s	=	specific entropy
$\vec{U}$	=	circumferential velocity vector
$\vec{V}$	=	absolute velocity vector
$\vec{W}$	=	relative velocity vector
Z	=	loss coefficient
α	=	absolute flow angle (stator)
β	=	relative flow angle (rotor)
ϕ	=	flow coefficient
λ, ψ	=	polytropic, isentropic load coefficient
η	=	polytropic efficiency
χ	=	isentropic enthalpy difference
μ, ν	=	velocity ratios
σ	=	cascade solidity
ζ_t	=	total loss parameter

Subscripts

0	=	design point
$1,2,3$	=	station number
ax	=	axial component
m	=	modified (diffusion factor)
r	=	relative
s	=	isentropic value
t	=	total (loss coefficient)
u	=	circumferential component
∞	=	free stream inside the blade channel

Superscripts

$'$	=	stator value
$''$	=	rotor value

INTRODUCTION

During the off-design operation of a gas turbine engine, the compressor component may be subjected to extreme operating conditions. These conditions are generally associated with significant changes in the mass flow rate, temperature, and pressure. For a typical compressor stage, the change in mass flow rate affects the velocity diagram of the stage, which alters its efficiency, power consumption rate, and overall performance.

Presented at the International Gas Turbine and Aeroengine Congress and Exposition
Houston, Texas - June 5-8, 1995

Considerable deviation from the design point may cause the compressor component of a gas engine to enter into the post-stall regime. Operation of the compressor in the post-stall regime can take the form of either rotating stall or surge. The surge mode involves mass flow reversal within the compressor, leading to extreme mechanical loads on the compressor blades and may cause damages to the entire engine.

To properly design power generation and aero gas turbine engines, the designer needs accurate methods to predict the design point performance and efficiency for the entire engine. To assess the reliability of the design, however, the designer needs accurate and reliable methods to predict the relevant component's efficiency and performance over a wide range of off-design operating points. One of the critical issues facing the compressor designer is the operation of the compressor in the post-stall regime.

Although compressor off-design simulation has been attempted in the past, post-stall operation of the compressor has been a primary topic of compressor research. Several attempts were made by Greitzer (1976), Moore (1983, 1984), and Moore and Greitzer (1985) to predict the post-stall operation of axial compressors. The efforts ranged from a simple model, which included an actuator disk, duct, and throttable plenum (Greitzer 1976), to a set of three non-linear third order partial differential equations for pressure rise and flow coefficient. The solution of these equations attempted to predict the growth, and possible decay of rotating stall cells during a compressor transient (Moore, and Greitzer, 1985). Greitzer's efforts (1976) introduced the so-called B parameter, which is a function of the circumferential Mach number and the ratio of the plenum volume to the duct volume of the model. According to the study, the value of B indicates the possibility of rotating stall or surge occurring within the compressor. Compressor instabilities would occur for the B value in excess of 0.7. However, the prediction of the instabilities based on the B parameter does not rely on compressor stage parameters such as the stage load coefficient, stage flow coefficient, diffusion factor, or stage efficiency, but rather on components that do not exist in an actual engine. Davis and O'Brien (1987) presented a one-dimensional, stage-by-stage modeling technique solving the non-linear conservation equations. Furthermore, they used a set of quasi-steady-state stage characteristics modified by a first order lagging equation to simulate dynamic behavior. The majority of the work focused on the compressor as an individual component and did not relate it to the rest of the engine. An attempt to simulate the dynamic behavior of compressors as a part of the entire engine was made by Schobeiri (1985a, 1985b, 1985c, and 1986) in his code COTRAN. The code utilized compressor performance maps coupled with the governing differential equations of mass, momentum, energy, and moment of momentum to perform dynamic engine simulation.

The prerequisite for compressor dynamic simulation is a detailed knowledge of the design point properties as well as the overall performance characteristics. This information leads to knowledge of the off-design performance behavior. Two methods may be employed to gain this knowledge. The first and easiest method is to obtain the needed information by using the specific compressor operational map as provided by the engine manufacturer. If the information for the compressor of interest is available, however, it is typically proprietary. This leaves the analysis engineer with no way of gaining access to the data. The second method, discussed herein, is to perform a comprehensive row-by-row analysis of the flow within the compressor stages. Row-by-row analysis of the flow leads to the prediction of the off-design dynamic behavior of the compressor over a wide range of operating conditions. The objective of this article is to present a comprehensive and reliable method which is ultimately capable of utilizing one-dimensional row-by-row flow analysis to generate compressor performance maps. Using the geometry of the multistage compressor of a BBC power generation gas turbine engine, three different compressor performance maps are generated for low-pressure (LP), intermediate-pressure (IP) and high-pressure (HP) stage groups. The results are compared with the maps obtained from experiment.

ROW-BY-ROW COMPRESSOR CALCULATION

The row-by-row flow analysis method presented in this paper is equally applicable to axial and radial turbines and compressors, as reported by Schobeiri (1990a, 1990b, and 1992a), and Schobeiri and Abouelkheir (1992b). This method is based on a one-dimensional calculation of the compression process using a set of dimensionless stage characteristics. These stage characteristics, along with a comprehensive loss correlation developed by Schobeiri (1987, 1994) describe the design and off-design behavior of the stage.

Stage Characteristics

The performance behavior of the compressor stage is completely described by the stage characteristics. The meridional view, blade configuration, and velocity diagram of a typical compressor are shown in Fig. 1. To begin the analysis, the following dimensionless are

introduced and used in conjunction with the velocity diagram in Fig. 1c:

$$\phi = \frac{V_{ax3}}{U_3}\ ,\ \mu = \frac{V_{ax2}}{V_{ax3}}\ ,\ r = \frac{\Delta h''}{\Delta h'' + \Delta h'}$$

$$\nu = \frac{U_2}{U_3}\ ,\ \lambda = \frac{\Delta H}{U_3^2} = \frac{U_2 V_{u2} + U_3 V_{u3}}{U_3^2}$$

$$R = \frac{\rho_2}{\rho_3} = \frac{b_3 D_3}{b_2 \mu D_2} \qquad (1)$$

These dimensionless variables are incorporated into the conservation equations of mass, momentum, moment of momentum, and energy. The compressor stage behavior is completely determined from the following set of four equations shown by Schobeiri (1990a, 1990b, and 1992a), and Schobeiri and Abouelkheir (1992b):

$$\cot\alpha_2 - \cot\beta_2 = \frac{\nu}{\mu\,\phi} \qquad (2a)$$

$$\cot\alpha_3 - \cot\beta_3 = \frac{1}{\phi} \qquad (2b)$$

$$\lambda = \phi\,(\,\mu\nu\cot\alpha_2 - \cot\beta_3\,) - 1 \qquad (2c)$$

$$r = 1 + \frac{\phi^2}{2\lambda}\,[\,1 + \cot^2\alpha_3 - \mu^2\,(\,1 + \cot^2\alpha_2\,)\,] \qquad (2d)$$

Considering the above equations, two methods may be used for calculating the row-by-row compression. The first method uses an alternating frame of reference so that the absolute and relative quantities are called upon in an alternating manner. The second method simultaneously uses both absolute and relative quantities. Both methods are equivalent and represent the same physical fact. The second method has proven to be more CPU-time effective as shown by Schobeiri, and Abouelkheir (1992b).

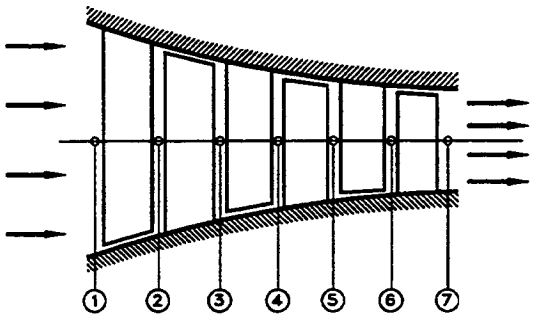

A) MERIDIONAL VIEW

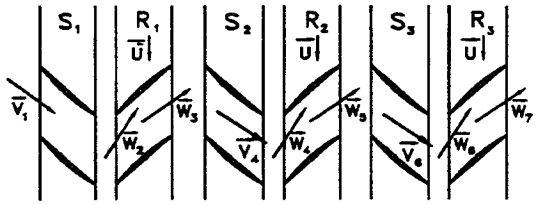

B) BLADE CONFIGURATION

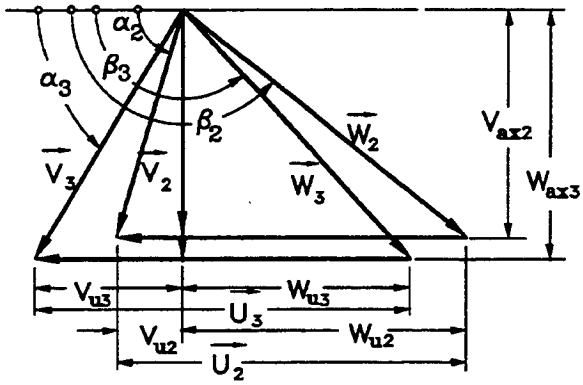

C) VELOCITY DIAGRAM

FIG. 1 MERIDIONAL VIEW, BLADE CONFIGURATION, AND VELOCITY DIAGRAM OF A TYPICAL COMPRESSOR

Row-by-Row Compression Process

The total energy equation for an adiabatic system states that the total enthalpy within the system is constant. This equation may be written both in absolute and relative frames of references. This leads to the following expressions for the polytropic and isentropic enthalpy differences within the stator and rotor, as shown in Fig. 2:

$$\Delta h' = h_1 - h_2 = \frac{1}{2}\left(V_2^2 - V_1^2 \right) \quad (3)$$

$$\Delta h_s' = h_1 - h_{2s} = \frac{1}{2}\left(V_{2s}^2 - V_1^2 \right) \quad (4)$$

$$\Delta h'' = h_2 - h_3 = \frac{1}{2}\left(W_3^2 - W_2^2 + U_2^2 - U_3^2 \right) \quad (5)$$

$$\Delta h_s'' = h_2 - h_{3s} = \frac{1}{2}\left(W_{3s}^2 - W_2^2 + U_2^2 - U_3^2 \right) \quad (6)$$

The detailed compression procedure on the (h-s) diagram is presented in Fig. 2. Introducing the efficiency definition for the stator and rotor row, respectively:

$$\eta' = \frac{\Delta h_s'}{\Delta h'} \quad , \quad \eta'' = \frac{\Delta h_s''}{\Delta h''} \quad (7)$$

Incorporating Eq. (7) into Eqs. (3-6), the isentropic enthalpy difference for the stator and rotor row, respectively, may be expressed by:

$$\Delta h_s' = \frac{\eta'}{2}\left(V_2^2 - V_3^2 \right) \quad (8)$$

$$\Delta h_s'' = \frac{\eta''}{2}\left(W_3^2 - V_2^2 + 2V_{u2}U_2 - U_3^2 \right) \quad (9)$$

The expression for the dimensionless isentropic enthalpy difference is obtained by dividing Eqs. (8) and (9) by the circumferential kinetic energy at the exit of the stage. The expressions for the dimensionless isentropic enthalpy difference may be written in terms of the stage parameters of Eq. (1) that result in Eqs. (10) and (11). Further analysis of Eqs. (10) and (11) shows that knowing of the entire stage parameters is necessary to determine the row isentropic enthalpy difference, which

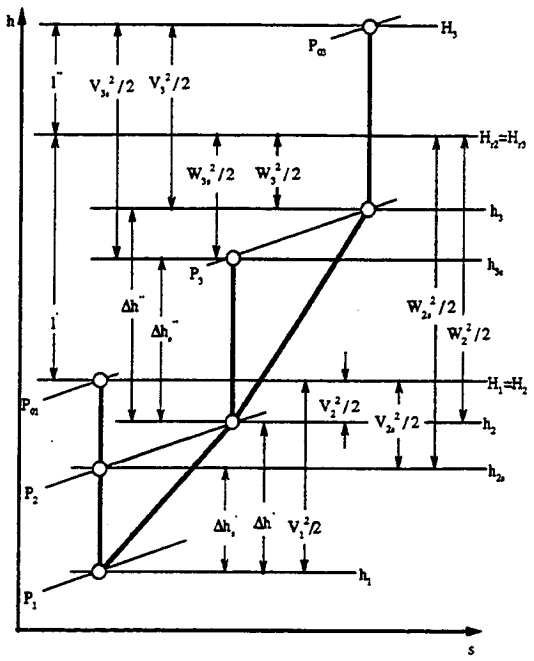

FIG. 2 DETAILED h-s COMPRESSION DIAGRAM OF A TYPICAL COMPRESSOR STAGE

$$\chi' = \frac{\Delta h_s'}{U_3^2} = \frac{\eta'}{2}\left[\frac{\phi^2\mu^2}{\sin^2\alpha_2} - \frac{\phi^2}{\sin^2\beta_3} - 2\phi\cot\beta_3 - 1 \right] \quad (10)$$

$$\chi'' = \frac{\Delta h_s''}{U_3^2} = \frac{\eta''}{2}\left[\frac{\phi^2}{\sin^2\beta_3} - \frac{\mu^2\phi^2}{\sin^2\alpha_2} + 2\phi\mu\nu\cot\alpha_2 - 1 \right] \quad (11)$$

requires many iterations. To avoid an iterative procedure, we use a row-by-row calculation method requiring virtual division of the stage specific mechanical energy (Schobeiri, and Abouelkheir, 1992b). The stage specific polytropic mechanical energy l, as well as the isentropic mechanical energy l_s are subdivided into stator, and rotor contributions, which can also be seen in Fig. 2:

$$l' = \frac{1}{2} V_2^2 - \frac{1}{2} W_2^2 \quad (12)$$

$$l'_s = \frac{1}{2} V_{2s}^2 - \frac{1}{2} W_2^2 \quad (13)$$

$$l'' = \frac{1}{2} (W_3^2 - U_3^2 + U_2^2 - V_3^2) \quad (14)$$

$$l''_s = \frac{1}{2} (W_{3s}^2 - U_3^2 + U_2^2 - V_3^2) \quad (15)$$

Using the polytropic specific mechanical energy expressions given in Eqs. (12,14) and dividing them by the circumferential kinetic energy at the exit of the individual row, the dimensionless row polytropic load coefficients for stator and rotor are:

$$\lambda' = \frac{l'}{U_2^2} = \phi' \cot \alpha_2 - \frac{1}{2} \quad (16)$$

$$\lambda'' = \frac{l''}{U_3^2} = - \phi'' \cot \beta_3 - 1 + \frac{v^2}{2} \quad (17)$$

where, $\phi' = V_{ax2} / U_2$, and $\phi'' = V_{ax3} / U_3$.

Combining Eqs. (12) - (15) with the efficiency definition for the stator and rotor rows, Eq. (7), the following expressions for the efficiency are obtained:

$$\eta' = \frac{2l'_s - 2l' + V_2^2 - V_1^2}{V_2^2 - V_1^2} \quad (18)$$

$$\eta'' = \frac{2l''_s - 2l'' + W_3^2 - W_2^2}{W_3^2 - W_2^2} \quad (19)$$

The isentropic row load coefficient ψ is defined as the dimensionless isentropic specific mechanical energy for the row. Non-dimensionalizing the efficiency expressions above, multiplying and dividing by the circumferential kinetic energy at the exit of the row, the isentropic row load coefficients for the stator and rotor rows are obtained:

$$\psi' = \frac{l'_s}{U_2^2} =$$

$$\lambda' + \left(\frac{\phi'^2}{2\sin^2\alpha_2} - \frac{\phi'^2}{2\mu^2\sin^2\alpha_3}\right) (\eta' - 1) \quad (20)$$

$$\psi'' = \frac{l''_s}{U_3^2} =$$

$$\lambda'' + \left(\frac{\phi''^2}{2\sin^2\beta_3} - \frac{\phi''^2\mu^2}{2\sin^2\beta_2}\right) (\eta'' - 1) \quad (21)$$

All the information necessary to pursue the compression process on the h-s diagram is now available to predict the compressor behavior with sufficient accuracy and reliability. Given the pressure and temperature at the inlet, the remaining thermodynamic properties are calculated using the state equation of the gas. The row flow coefficient, ϕ, is calculated from the continuity equation:

$$\phi = \frac{V_{ax}}{U} = \frac{\dot{m}}{\rho A U} = \frac{\dot{m}}{\rho A \omega R} \quad (22)$$

Given the exit stator and rotor blade angle (α_2, β_3) as input data necessary to describe the geometry and the above flow coefficient, we determine the flow angles (α_3, β_2) for the stator and rotor rows, respectively:

$$\beta_2 = \tan^{-1} \frac{\phi'}{\phi' \cot \alpha_2 - 1} \quad (23a)$$

$$\alpha_3 = \tan^{-1} \frac{\phi''}{\phi'' \cot \beta_3 + 1} \quad (23b)$$

Upon determining all the angles involved in the velocity diagram, the velocities and their components are fully known. The velocity triangle at the exit of the row is calculated and the flow behavior is completely described by the velocity diagram. The flow coefficient, ϕ' and ϕ'', and the flow angles (α_3, β_3, α_2, β_2,) are necessary tools to determine the polytropic and isentropic enthalpy

differences between the inlet and exit of the row. The amount of work consumed by the flow to increase its pressure and temperature is represented by the polytropic load coefficients, λ', λ'', and the isentropic load coefficients ψ', ψ'' as presented above. Finally, from the energy balance relationships, the complete compression process for the stage is determined by the following set of equations:

$$h_2 = h_1 - l' - \frac{1}{2}\left(W_2^2 - V_1^2 \right) \qquad (24a)$$

$$h_{2s} = h_1 - l'_s - \frac{1}{2}\left(W_2^2 - V_1^2 \right) \qquad (24b)$$

$$h_3 = h_2 - l'' - \frac{1}{2}\left(V_3^2 - W_2^2 \right) \qquad (24c)$$

$$h_{3s} = h_2 - l''_s - \frac{1}{2}\left(V_3^2 - W_2^2 \right) \qquad (24d)$$

The above procedure can be easily repeated for all the stages of the compressor in question. However, it should be pointed out that the above analysis is completely dependent on an accurate and reliable method for determining the off-design efficiency. This is the subject of the next section.

Off-Design Efficiency Calculation

The off-design efficiency calculation is based on the analysis of the diffusion factor. Several expressions for the diffusion factor exist, as shown by Lieblein et al. (1953), and Seyler and Smith (1967). However, Schobeiri's (1987, 1994) expression for the diffusion factor was most suitable for the analysis at hand. The modified diffusion factor expression by Schobeiri includes compressibility effects and, therefore, is capable of handling highly compressible flow such as in transonic compressors. This expression is:

$$D_m = 1 - \frac{W_{ex}}{W_{in}} + \frac{R_{ex}V_{u,ex} - R_{in}V_{u,in}}{\sigma\left(R_{in} + R_{ex} \right) W_{in}} \left(\frac{\rho_\infty}{\rho_{in}} \right) \qquad (25)$$

where the subscripts (in, ex) refer to the inlet and exit of the blade, respectively. To apply the above diffusion factor definition to stators and rotors on an individual basis, separate expressions were derived in terms of known stage and row quantities. The expression for the stator row given by Schobeiri (1987, 1994) is:

$$D'_m = 1 - \frac{\sin\alpha_1}{\mu\sin\alpha_2} + \frac{\sin^2\alpha_1}{2\sigma}\left(\cot\alpha_1 - \frac{\cot\alpha_2}{\mu\nu} \right) \cdot \left[1 - M_1^2 \left(\frac{\sin\alpha_1}{\mu\sin\alpha_2} \right)\left(\frac{\sin\alpha_1}{\mu\sin\alpha_2} - 1 \right) \right] \qquad (26)$$

and for the rotor row:

$$D''_m = 1 - \frac{\sin\beta_2}{\mu\sin\beta_3} + \frac{\sin^2\beta_2}{2\sigma}\left(\frac{1 - \nu^2}{\mu\nu\phi''} + \cot\beta_2 - \frac{\cot\beta_3}{\mu\nu} \right) \cdot \left[1 - M_1^2 \left(\frac{\sin\beta_2}{\mu\sin\beta_3} \right)\left(\frac{\sin\beta_2}{\mu\sin\beta_3} - 1 \right) \right] \qquad (27)$$

Using the above modified diffusion factor, a new total loss parameter correlation was presented in the study by Schobeiri (1987, 1994). For the sake of completeness, the total loss parameter is replotted in Fig. 3 as a function of the modified diffusion factor with the immersion factor, defined in Fig. 3a, as a parameter. As shown in Fig. 3b, a set of curves representing the blade total loss parameter $\zeta t \sin(\alpha_{in}, \beta_{in})/2\sigma$ is plotted, with α_{in}, β_{in} as the inlet flow angle of stator or rotor row and σ as the blade solidity ratio. These curves were fitted and may be presented in the form of polynomials of the modified diffusion factor. The coefficients of the resulting polynomial equations are presented in Table 1. The efficiency is defined in terms of the loss coefficient Z, which is a function of ζ_t and may be written for the stator and rotor, respectively:

$$Z'_t = \frac{\zeta'_t V_1^2}{2 l'} = \frac{\zeta'_t \phi''^2}{2 \lambda' \nu^2 \left(\sin^2 \alpha_3 \right)} \qquad (28)$$

$$Z''_t = \frac{\zeta''_t W_2^2}{2 l''} = \frac{\zeta''_t \phi'^2 \nu^2}{2 \lambda'' \left(\sin^2 \beta_2 \right)} \qquad (29)$$

Finally, the row efficiency can be expressed as:

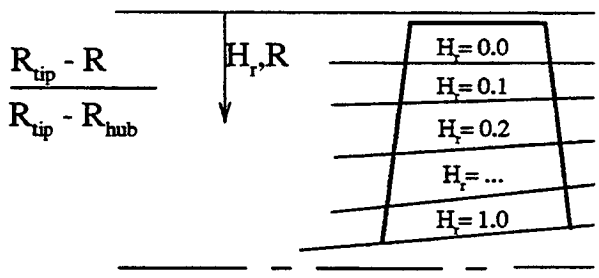

A) IMMERSION FACTOR DEFINITION

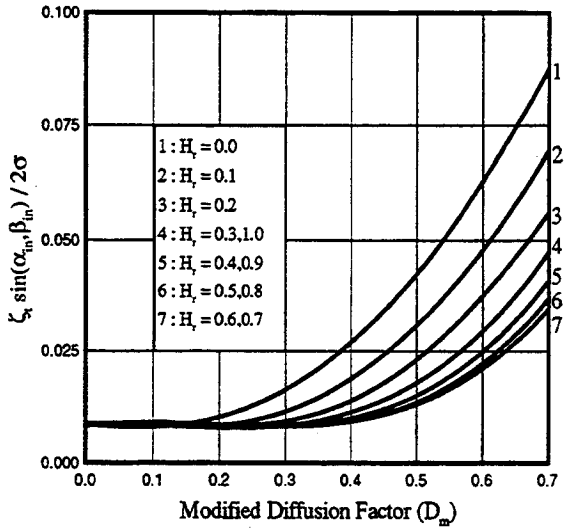

B) TOTAL LOSS PARAMETER AS A FUNCTION OF D_m.

FIG. 3 IMMERSION FACTOR DEFINITION, AND TOTAL LOSS PARAMETER AS A FUNCTION OF THE MODIFIED DIFFUSION FACTOR D_m, WITH IMMERSION FACTOR AS PARAMETER, Schobeiri (1994).

$$\eta' = 1 - Z_t' \quad , \quad \eta'' = 1 - Z_t'' \qquad (30)$$

The loss parameter curves of Fig. 3b are not symmetric and, therefore, must be applied to the blade in a manner compatible with their distribution over the blade spanwise direction. For this purpose we apply energy balance to the blade, which results in:

$$\sum_{j=1}^{n} \dot{m}_j \left(\frac{\Delta h_{sj}}{\eta_j} \right) = \dot{m} \left(\frac{\Delta h_s}{\eta} \right) \qquad (31)$$

where the index j refers to the blade from tip to hub. Eq. (33), coupled with the total loss definition, can be reduced to:

$$Z_t = \frac{1}{\Delta h_s A_t} \left(\sum_{j=1}^{n} \Delta h_{sj} A_j Z_j \right) \qquad (32)$$

The above formulation of the loss parameter distribution in the spanwise direction is required by the one-dimensional row-by-row analysis presented in this paper.

CALCULATION RESULTS

To test the reliability of the presented analysis, the multistage compressor of a BBC-gas turbine engine was chosen because its geometry and experimental performance maps of its high-pressure (HP), intermediate-pressure (IP), and low-pressure (LP) stage groups are documented and are reported in the study by Klingenböck and Rappard (1977). Given only the compressor geometry, steady state calculations were performed by varying the rotational speed and mass flow rate. The choke line was predicted by monitoring the local Mach number. Starting from a given constant rotational speed and mass flow (point 1 in Fig. 4), the compressor performance curve was calculated by continuously decreasing the mass flow. As expected, the mass flow reduction caused an increase of the blade load coefficient within the pre-stall regime and resulted in a higher pressure ratio. After passing through the design point (point 2) by further decreasing the compressor mass flow rate, a dip was noticed in the pressure ratio curve, followed by a seemingly discontinuous decrease of the pressure ratio at point 3. This point, which has approximately a zero-slope, indicates a possible inception of rotating stall and surge. A further reduction of mass flow beyond point 3 may enter the compressor into a post stall regime, which can only be simulated dynamically. Figure 4 exhibits a wide range of off-design operation, including the possible inception of rotating stall and surge. The above analysis was further carried out at several different rotational speeds to obtain the complete compressor performance map. The common factor for all the dips in the performance line was that they all occurred

TABLE 1 POLYNOMIAL COEFFICIENTS FOR THE LOSS PARAMETER CURVES IN TERMS OF THE MODIFIED DIFFUSION FACTOR D_m.

Polynomial coefficients for the loss parameter curves						
Curve No.	Coeff. for D_m^0	Coeff. for D_m^1	Coeff. for D_m^2	Coeff. for D_m^3	Coeff. for D_m^4	Coeff. for D_m^5
1	0.008576	-0.01228	0.02937	0.4350	-0.41499	0.13919
2	0.008565	0.014185	-0.24764	1.07477	-1.15633	0.483076
3	0.008459	0.015972	-0.16958	0.419837	0.065103	-0.23947
4	0.008744	0.002338	-0.07784	0.21905	0.0	0.0
5	0.008448	0.014825	-0.12485	0.242714	0.0	0.0
6	0.008247	0.019457	-0.13932	0.24268	0.0	0.0
7	0.008279	0.016187	-0.11357	0.186606	0.027259	0.0

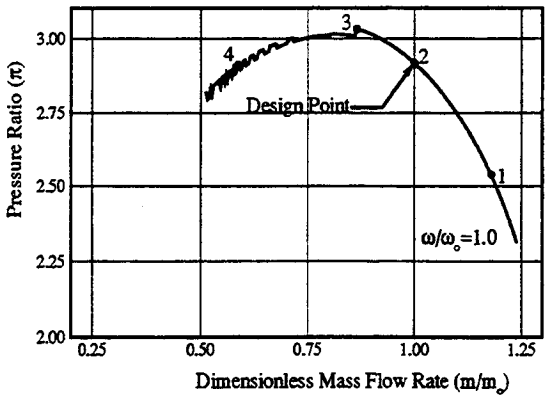

FIG. 4 COMPRESSOR MAP ILLUSTRATING ROTATING STALL AND SURGE INSTABILITIES

within a modified diffusion factor range of 0.6 to 0.7.

Utilizing the above diffusion factor information as a criterion for predicting the surge margins, performance maps were generated for HP-, IP-, and the LP-compressor stage groups of a BBC- power generation gas turbine. Starting from the low pressure stage group, Fig. 5 exhibits the relative pressure ratio π/π_o versus the dimensionless mass flow ratio $\dot{m}/\dot{m}_o$ with the rotational speed ratio ω/ω_o as parameter. The reference quantities π_o, m_o and ω_o refer to the design pressure ratio, design mass flow, and design angular velocity, respectively.

The calculated performance curves, displayed by solid lines, were obtained using the row-by-row calculation method presented in this paper. To cover a wide operation range, the relative speed was varied from ω/ω_o = 0.3 to 1.1. The surge limit in Fig. 5 was obtained by considering the previously mentioned diffusion factor criterion of 0.6 to 0.7. The calculated performance curves are compared with the corresponding actual performance points reported by Klingenböck and Rappard (1977). As seen in Fig. 5, good agreement is found between the calculated and measured actual performance curves for a wide range of ω/ω_o = 0.4 to 0.8. Good agreement is also seen for $\dot{m}/\dot{m}_o$ less than 1, for the design speed curve with ω/ω_o = 1.0. However, approaching the choke line by increasing the mass flow exhibits a small deviation between the calculated and the measured points, which can be attributed to the assumption that the averaged deviation angle over the blade height may be of negligible magnitude (see the corresponding discussion at the end of this section).

The corresponding relative efficiency ratio η/η_o versus the relative pressure ratio π/π_o with the rotational speed ratio ω/ω_o as parameter is shown in Fig. 6 ,where the efficiency curves were non-dimensionalized by the reference design point efficiency η_o. The calculated efficiency curves, displayed by the solid lines, were obtained using the row-by-row calculation and theefficiency correlations mentioned previously. As

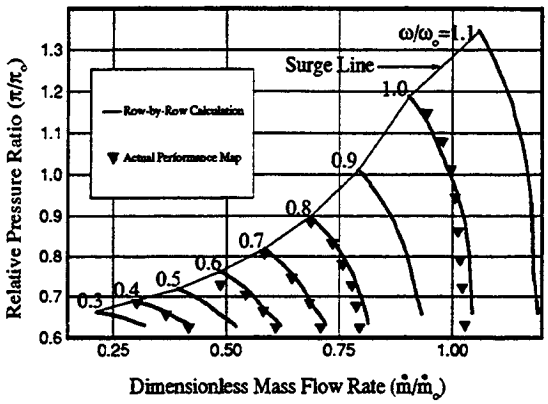

FIG. 5 LOW PRESSURE COMPRESSOR RELATIVE PRESSURE RATIO AS A FUNCTION OF DIMENSIONLESS MASS FLOW RATE

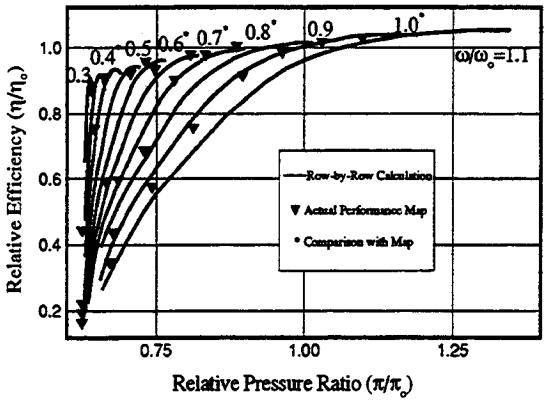

FIG. 6 LOW PRESSURE COMPRESSOR RELATIVE EFFICIENCY AS A FUNCTION OF THE RELATIVE PRESSURE RATIO

discussed previously, to cover a wide operation range, the relative speed was varied from ω/ω_0 = 0.3 to 1.1. These curves are compared with the corresponding actual efficiency data obtained form experiments that were available for ω/ω_0 = 0.4, 0.6, 0.7,0.8, and 1.0 labeled with * as shown in Fig. 6. As can be seen, a relatively good agreement between the calculated and measured actual efficiency curves are found for higher η/η_0 values for a wide range of ω/ω_0. However, for lower η/η_0 values, as a result of higher mass flows, the comparison between the calculated and the measured efficiency points reveals a slight deviation. As discussed previously, this deviation might be attributed to the loss correlation, neglecting the averaged deviation angle.

Similar satisfactory results were obtained by applying the presented row-by-row calculation method to the IP- and HP- compressor stage groups. Since the calculation results for the HP- stage group is similar to the IP- stage group, we present only the IP-performance results. The performance maps are shown in Figs. 7 and 8, where the calculated results are compared with the experimentally obtained performance map. Similar to the previous LP-case, wide operation range is covered by varying the relative speed from ω/ω_0 = 0.3 to 1.1. The surge limit shown in Fig. 7 was obtained by considering same diffusion factor criterion mentioned earlier. The calculated performance curves are compared with the corresponding actual performance points reported by Klingenböck and Rappard (1977). Unlike the LP-case, for the IP-stage group experimental data were available only for ω/ω_0 = 0.6, 0.7, 0.8, and 1.0 as shown in Fig. 7. As seen in Fig. 7, satisfactory agreement between the calculated and measured actual performance curves is found for ω/ω_0 = 0.6, 0.7, and 0.9. For the design speed curve with ω/ω_0 = 1.0, excellent agreement is also seen for $\dot{m}/\dot{m}_0$ less than 1. However, approaching the choke line by increasing the mass flow exhibits a minor deviation between the calculated and the measured points. This deviation is much smaller than the LP case. Good results are also seen for the efficiency curves plotted in Fig. 8.

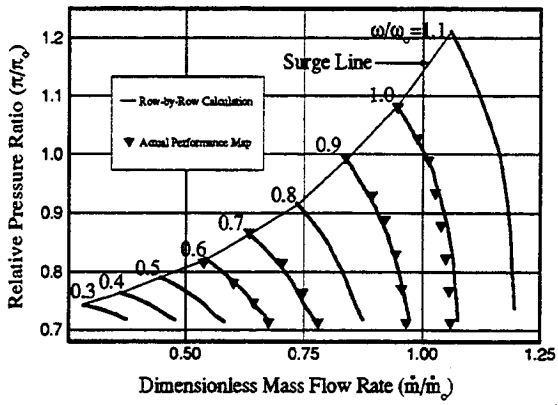

FIG. 7 INTERMEDIATE PRESSURE COMPRESSOR RELATIVE PRESSURE RATIO AS A FUNCTION OF THE DIMENSIONLESS MASS FLOW RATE

Analyzing the LP-, IP-, and HP- performance results and comparing them with experimentally determined performance maps leads to the conclusion that the efficiency calculation for IP- and HP- compressor stage groups with relatively smaller blade heights are better predicted by the correlation used in this paper. It should be pointed out that by averaging the loss coefficient over the blade height, the averaged deviation angle was assumed to be negligibly small, which accounts for the cancellation of the hub and tip effect on the averaged deviation angle. This assumption, however, may not be applicable to the low pressure part, where the averaged deviation angle may have non-negligible values due to strong three dimensional effects.

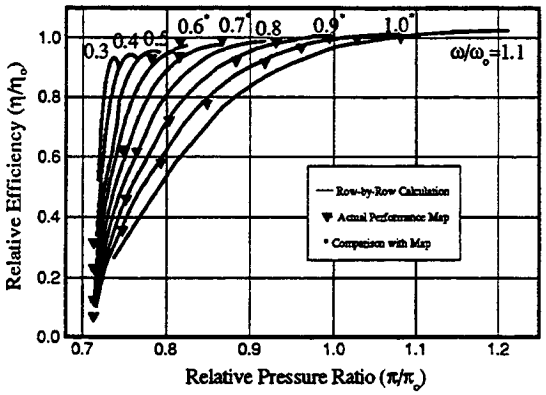

FIG. 8 INTERMEDIATE PRESSURE COMPRESSOR RELATIVE EFFICIENCY AS A FUNCTION OF THE RELATIVE PRESSURE RATIO

CONCLUSION

A row-by-row off-design calculation method is presented for the prediction of the performance behavior of compressors under extreme off-design conditions. The off-design efficiency is calculated using a modified diffusion factor with compressibility effects. The method is applied to the LP-, IP-, and HP- compressor stage groups of a BBC- power generation gas turbine engine for which the performance map was calculated. The results of the presented row-by-row calculation method were compared with the actual compressor performance map obtained from the experiment. For all three compressor groups a good agreement was shown to within 4%.

ACKNOWLEDGEMENT

The authors would like to express their sincere thanks and appreciations to Mr. Carl Lorenzo, Chief Systems Dynamics Branch and Dr. Dan Paxson and the administration of the NASA Lewis Research Center for the continuous cooperation and support of this project. The second author would like to thank ABB (former BBC), Gas Turbine Division and his Colleague Dr. H. Stoff for permitting the simulation of the compressor presented in this paper.

REFERENCES

Davis, M. W., and O'Brien, W. F., 1987, "A Stage-by-Stage Post-Stall Compression System Modeling Technique", presented at the AIAA/SAE/ASME/ASEE 23rd Joint Propulsion Conference, July, 1987, San Diego, California, AIAA-87-2088.

Greitzer, E. M., 1976, "Surge and Rotating Stall in Axial Flow Compressors, Part I: Theoretical Compression System Model", *ASME Transactions, Journal of Engineering for Power*, Vol. 98, pp. 190-198.

Klingenböck, U. Rappard, A. 1977 "Off-Design Computing System", Von Karman Lecture Series: Performance of Gas Turbines 1977-1978.

Lieblein, S., Schwenk, F., and Broderick, R. L., 1953, "Diffusion Factors for Estimating Losses and Limiting Blade Loadings in Axial Flow Compressor Blade Elements", NACA RM E53D01, June 1953.

Moore, F. K., 1983, "A Theory of Rotating Stall of Multistage Axial Compressors", NASA CR 3685.

Moore, F. K., 1984, "A Theory of Rotating Stall of Multistage Compressors, Part I, II, III", ASME *Journal of Engineering for Power*, Vol. 106, No. 2, April 1984, pp. 313-336.

Moore, F. K., and Greitzer, E. M., 1985, "A Theory of Post-Stall Transients in Multistage Axial Compression Systems", NASA CR 3878.

Schobeiri, T., 1985a, "Aero-Thermodynamics of Unsteady Flows in Gas Turbine Systems", Brown Boveri Company, Gas Turbine Division, Baden, Switzerland, BBC-TCG-51.

Schobeiri, T., 1985b, "COTRAN, the Computer Code for Simulation of Unsteady Behavior of Gas Turbines", Brown Boveri Company, Gas Turbine Division, Baden, Switzerland, BBC-TCG-53.

Schobeiri, T., 1985c, "Digital Computer Simulation of the Dynamic Response of Gas Turbines", *VDI - Annual Journal of Turbomachinery*, pp. 381-400.

Schobeiri, T., 1986, "A General Computational Method for Simulation and Prediction of Transient Behavior of Gas Turbines", ASME 86-GT-180.

Schobeiri, T., 1987, "Verlustkorrelationen für transonische Kompressoren", BBC-TN 87/20.

Schobeiri, T., 1990a, "Thermo-Fluid Dynamic Design Study of Single and Double-Inflow Radial and Single-Stage Axial Steam Turbines for Open-Cycle Thermal Energy Conversion Net Power-Producing Experiment Facility in Hawaii", *Journal of Energy Resources Technology*, March 1990, Vol. 112.

Schobeiri, T., 1990b, "Optimum Design of a Low-Pressure, Double-Inflow, Radial Steam Turbine for Open-Cycle Ocean Thermal Energy Conversion", ASME *Journal of Turbomachinery*, January 1990, Vol. 112.

Schobeiri, T., 1992a, "One-Dimensional Methods for Accurate Prediction of Off-Design Performance Behavior of Axial Turbines", ASME 92-GT-54, presented at the International Gas Turbine and Aero engine Congress and Exposition, Cologne, Germany, June 1-4, 1992.

Schobeiri, T., and Abouelkheir, M., 1992b, "Row-by-Row Off-Design Performance Calculation Method for Turbines", AIAA *Journal of Propulsion and Power*, Vol. 8, No. 4, pp. 823-828.

Schobeiri, M. T., 1994, "New Loss Correlations for Compressors", under preparation.

Seyler, D. R., and Smith, Jr., L. H., 1967, "Single Stage Experimental Evaluation of High Mach Number Compressor Rotor Blading, Part I: Design of Rotor Blading", NASA CR 54581, April 1, 1967.